ENHANCING AERODYNAMIC PERFORMANCES OF HIGHLY LOADED COMPRESSOR CASCADE VIA GURNEY FLAP

Ramzi MDOUKI[1], Gérard BOIS[2], Abderrahmane GAHMOUSSE[3]

This paper was carried out to report numerical results on using Gurney flap to improve aerodynamic performance of linear highly loaded compressor cascade. The effects of location, slope and height of this passive device were investigated by optimal analysis. The obtained results revealed that the best Gurney flap achieved deflection enhancement and controlled boundary layer separation. Unfortunately, this improvement was accompanied with a penalty in total losses. While the relative rise of total loss coefficient was marked for the best controlled configuration particularly in design point, the Gurney flap could possibly be implemented by a semi-passive technique. It might be retracted when the separation is not occurred and deployed in the stall operation.

Keywords: 2D Cascade, Gurney Flap, Separation, Passive Control.

1. Introduction

The Gurney flap is a simple passive device used to enhance the lift coefficient of airfoils. It represents a rectangular flat plate attached to the wing pressure surface at the vicinity of the tailing edge. The gurney flap was used at first in 1960 for racing car wing by Daniel Gurney in order to improve the traction car by additional downward force and this idea was exploited after in aeronautical area by Lieback. As cited above, the Gurney flap produces an increasing in lift under influence of effective camber which depends principally to the flap height. The increasing in lift force with the addition of Gurney flap is accompanying with an increment in drag coefficient. Lieback suggested that the optimal flap height should be between the values 1 and 2 percent of the chord for admissible losses [1]. In the knowledge limits of the author, there have been a few papers which explore the effects of Gurney flap in turbomachinery field. Myose et al [2] studied the effect of Gurney flap in NACA 65(12)10 compressor cascade using tuft flow visualization in water table. At low Reynolds number a measurements

[1] PhD, Dept.of Mechanic, University LARBI TEBESSI of Tebessa, Algeria, e-mail: mdouki_ramzi@yahoo.fr
[2] Prof., Arts et Métiers ParisTech, CER de Lille, e-mail: Gerard.BOIS@ENSAM.EU
[3] Prof., Dept.of Mechanic, University LARBI TEBESSI of Tebessa, Algeria, e-mail: abdgah@yahoo.fr

were taken for a Gurney flap with a height of 2 percent of the cord length attached normally to the trailing edge of the cascade blades. The study provides only information about operating conditions and shows that the Gurney flap delays the stall at large incoming flow angles. Experimental investigation of the Gurney flap was conducted by Byerley et al [3] on turbine blades in linear cascade to control laminar separation. The Gurney flap was added to the pressure side close to the tailing edge. Five different sizes of the flaps, ranging from 0.6 to 2.7 percent of axial chord, were tested and the measurements showed that the flap with diameter greater than 3.9 mm (2.3% of axial chord) has the potential to eliminate the separation bubble. Li et al [4] examined the effects of Gurney flaps on a NACA 0012 by experimental measurements of surface pressure distributions and wake profiles and confirmed that the flat height of 2% of chord length, where the device remains within the boundary layer, provides the highest lift-to-drag ratio. Through the paper of Wang at al [7], they had carried out a review of the characteristics and mechanisms of lift enhancement applications by GF and its applications. They cited that the optimum design of GF, in external flow around isolated airfoil, was identified by the location at trailing edge, perpendicular to the chord and its height shouldn't be exceed 2% of chord length.

In fact, the decreasing of the weight and length of compressor leads to reduce the number of blades or stages and therefore raises the level of loading and diffusion on the bladings. With these conditions, the phenomenon of boundary layer separation can be occurred and the bladings lose their performances. The use of control techniques becomes necessary to manipulate the boundary layer and eliminate or mitigate the detachment zones. In this present exploration the pivotal purpose is to carry out a parametric study to provide computational data on the performance of the Gurney flap in linear compressor cascade to control stalled high cambered blades NACA65(15)10. Three parameters are tested; location, slope and height of Gurney flap in order to identify the optimal flap configuration and determine its effect on the aerodynamic performances of cascade. The computations of the clean cascade are validated with experimental data performed in NASA by Emery et al [5].

2. Investigation with clean cascade and validation code results

The geometry and grid are built in the pre-processor GAMBIT. The computational geometry represents one flow passage in linear cascade of axial compressor, fig.1, (left). It is limited by four boundaries; inlet, outlet and two periodics. The inlet and outlet are positioned at approximately 1.7 and 2.0 chord lengths upstream and downstream from the leading edge and trailing edge, respectively. The distance between the two interfaces defines the cascade pitch s which is identified by the solidity $\sigma=c/s=1.00$. Within this study domain, the high

loaded blade NACA 65(15)10 has been chosen. The operating conditions are set at free-stream Mach number M=0.085 and Reynolds number Re_c=245000. Based on the data taken from the reference of Abbot [8] a program was developed to generate the coordinates of the NACA blade profile. Eight cascade configurations are developed by using different values of the stagger angle. Therefore, the blades cascade is characterized by a chord length c=0.127m and the following stagger angles $\lambda=18^0$, 20^0, 22^0, 24^0, 28^0, 30^0, 34^0 and 38^0. In the right of the figure 1, all details of cascade geometry are given; camber angle φ, camberline slopes at leading and trailing edges φ_1 and φ_2, respectively, incidence angle i, deviation angle δ, inflow angle β_1 , outflow angle β_2, stagger angle λ, pitch cascade s and blade chord c.

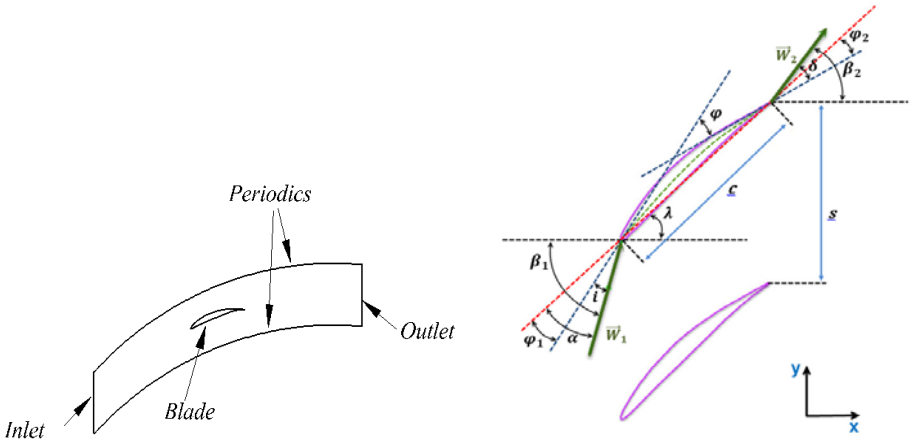

Fig. 1. Domain geometry (left) and details of cascade geometry (right)

Concerning the mesh, an O block configuration is applied around the blade. Two types of grid are used, a structured grid in the vicinity of blade surfaces to detect the severe gradients in the boundary layer zones and an unstructured grid with triangular cells in the remainder of computational domain. In order to resolve the whole boundary layer the first nodes near the blade surface are located at the position leading to y^+ less than 1 with a normal spacing expansion rate of 1.1 to guarantee the good capture of flow characteristics in the boundary layer. The total number of the cells for the cascade configuration is about 30000.

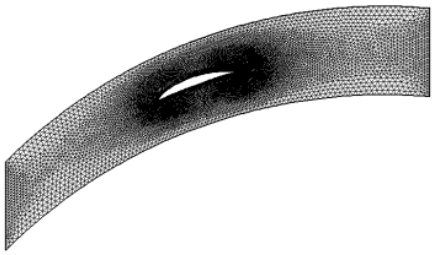

Fig. 2. Computational grid

The governing equations are discretized using the finite volume method applied in FLUENT solver. The second order spatial discretization scheme is used for continuity and momentum equations. The system of nonlinear equations is solved by a pressure-based approach. As the flow is considered as incompressible, no equation of state exists for pressure and SIMPLE algorithm is used to enforce the pressure-velocity coupling. At the upstream inlet boundary, the velocity and flow angle of the free-stream take the values, W_1=28.95 m/s and $\beta_1=45^0$, respectively. Furthermore, it was assumed that the turbulence intensity of the inlet flow is 1%. At the downstream outlet, the static pressure is imposed as atmospheric pressure. The velocity components and turbulence parameters are extrapolated from neighboring interior cells. The airfoil is modeled as viscous flow with no slip conditions imposed. The two interfaces are treated as periodic where the principle of ghost cells is introduced. During the calculations, the residuals are monitored. When the residuals go down at least 10^{-5}, the calculations are considered to be converged.

In order to validate the computational results, three experiment curves, comes from the Emery's report [5], are exploited to carry out this task. The first comparison is shown in Fig. 3 for the pressure evolution on the surface blade in terms of relative dynamic pressure, $S=2(P_{01}-P)/(\rho W_1^2)$. This comparison is performed for the stalled cascade configuration with angle of attack $\alpha_1=27^0$, a stagger angle $\lambda=18^0$ and solidity σ=1.00. Three models are tested for turbulence closure; Spalart-Allmaras, K-epsilon realizable and K-omega SST.

The two first models lead approximately to a same curve of the relative dynamic pressure S and give a good agreement with experiment than K-omega SST model, fig.3. Therefore, the Spalart-Allmaras model with one equation will be chosen due to its compromise between accuracy and computing costs and its robustness to model turbulent boundary layer flows on grid with high refinement near wall regions.

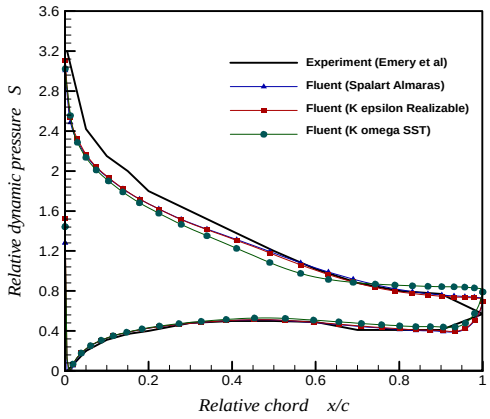

Fig. 3. Comparison between experimental and numerical results for the stalled cascade configuration ($\alpha_1=27^0$, $\lambda=18^0$, $\sigma=1.00$)

The second comparison represents the characteristic curves of turning angle $\theta=\beta_1-\beta_2$ and total loss pressure $\varpi=2(P_{t1}-P)/(\rho W_1^2)$ over the range of the angle of attack limited between 7^0 and 27^0 (fig. 4). The obtained results in figures 4 show a good agreement with the NASA test results found in [5], except loss coefficient values which are found higher over the entire range than measured data due to the fully turbulent treatment given to the flow in the computational procedure. Furthermore, our calculations are in 2D one and the experiments are done in a real cascade with a specific aspect ratio which is not the case for 2D calculations.

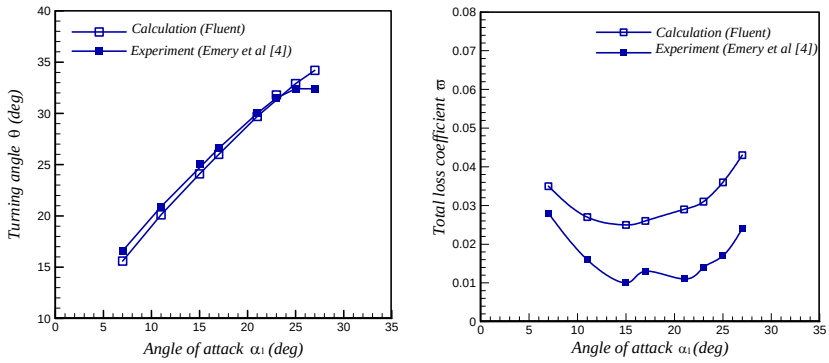

Fig. 4. Comparison between experimental and numerical results for different angles of attack, (turning angle-left, total loss pressure-right)

3. Investigation with controlled cascade and parametric study

Fig. 5 reveals three influence parameters; GF location X=x/c, GF height H=h/c and GF mounting angle φ. Each parameter is optimized in order to obtain

the best configuration. In this study, the thickness of the Gurney flap is equal to 0.1% of the chord length. The efficiency of control is analyzed in the basis of the mass averaged total loss coefficient, turning angle. Moreover, streamlines colored by axial velocity are represented to visualize the flow field and the separation zone and show the effect of the Gurney flap to control the stalled blading. In the cascade with GF, the mesh is generated of the same manner in the clean case. The figure 6 shows the grid near the region of the Gurney flap for the flapped cascade with X=0.95, φ=90^0, and H=0.01.

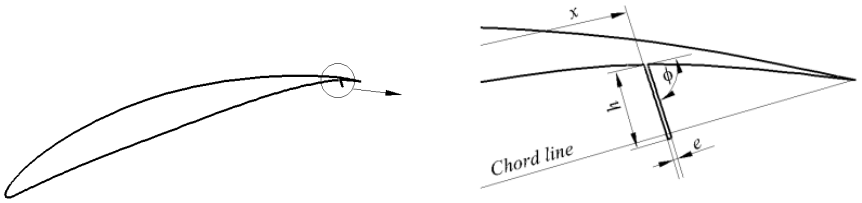

Fig. 5. Flapped Blading (left), Gurney flap details (right)

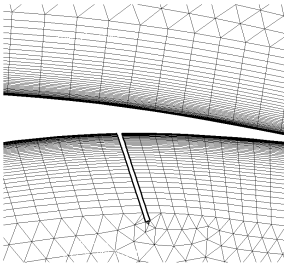

Fig. 6. Computational mesh for the controlled cascade near GF with X=0.95, φ=90^0, and H=0.01

This first part of the parametric study has the aim to analyze the effect of the Gurney flap location. Four cascade configurations with Gurney flap are chosen. The locations take the values X=0.85, 0.90, 0.95 and 1.00. The mounting angle φ and the height H of the Gurney flap are fixed with the values 90^0 and 0.02, respectively. In Fig. 7 which illustrates the influence of the Gurney flap on aerodynamic performances, the potential of the Gurney flap appears in the cases corresponding to the two mounting locations X=0.95 and X=1.00 with an increasing of 1^0 and 6^0 in turning angle, respectively. Concerning the total loss coefficient, all the controlled configurations mark an increasing in the level of losses. However, the values of losses for the different mounting locations remain close to the clean case. The axial velocity cartographies represented in figure 8 show that the separation zone developed on the extrados could be enlarged when the GF is shifted forward away from the trailing edge. Therefore, the trailing edge is chosen as optimal location.

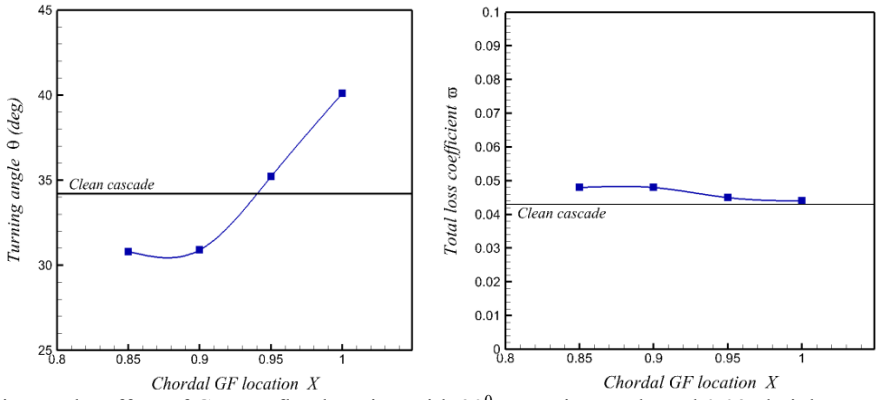

Fig. 7. The effect of Gurney flap location with 90^0 mounting angle and 0.02c height on turning angle -left and total loss pressure-right

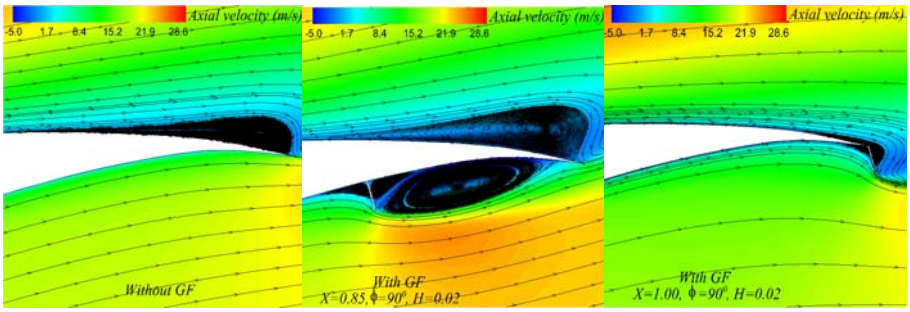

Fig. 8. Axial velocity contours and streamlines for clean and controlled cascades for two mounting locations (X=0.85 and 1.00)

The study of the GF mounting angle influence is performed in this section by fixing the GF chordal location and height as X=1.00 and H=0.02. Five values of the Gurney flap slope are used $\varphi=30^0$, 45^0, 60^0, 90^0 and 120^0. φ is defined as the angle between the chord line and the Gurney flap. According the turning angle evolution with the different values of the angle φ, as illustrated in the figure 9, it seems that all configurations give an enhancement compared to a clean cascade.

In particular, the angle $\varphi=90^0$ represents the optimal slope of GF in term of turning angle. The total losses, in the left of figure 9; oscillate around the clean case losses value between 0.042 and 0.045. Therefore, the slope $\varphi=90^0$ leads to losses penalty associated with turning angle improvement, although this penalty can be considered as negligible ($\delta(\varpi)\approx 2\%$), where $\delta(\varpi)$ is the relative rise in the total loss coefficient. The separation point in all controlled configurations is delayed, as it shown in the fig.10. Moreover, it can be clearly seen in figure 10 that the flow along flapped blading surfaces present improvements compared with

the corresponding blade rows acting without Gurney flap. The angle $\varphi=90^0$ is considered as the best mounting angle of GF.

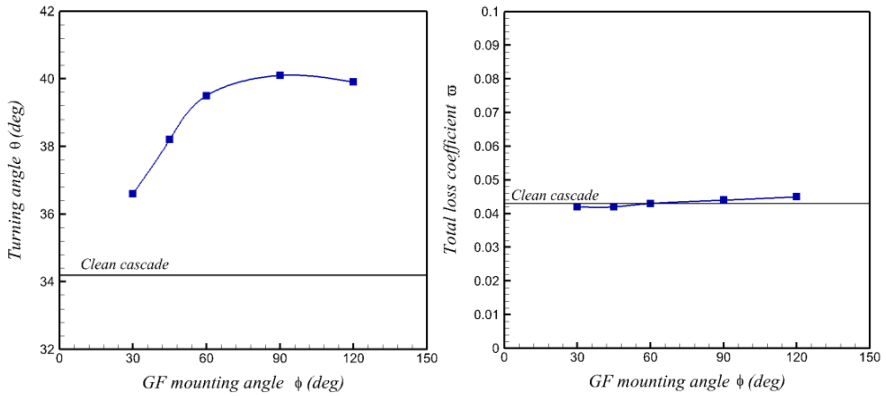

Fig. 9. The effect of Gurney flap mounting angle with trailing edge location and 0.02c height on turning angle-left and total loss pressure-right

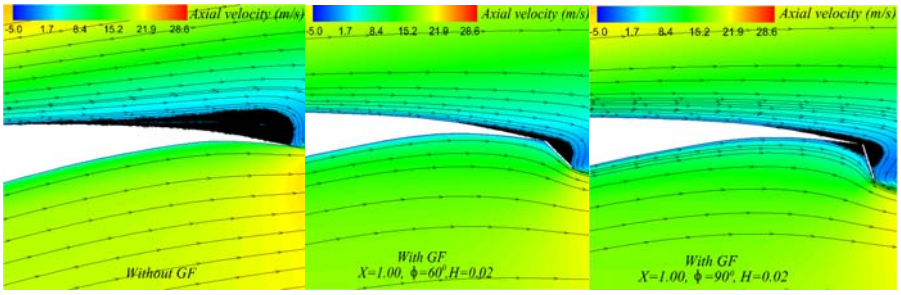

Fig. 10. Axial velocity contours and streamlines for clean and controlled cascades for two mounting angles ($\varphi=60^0$ and 90^0)

Similarly, in order to investigate the effect of GF height, which represents a key parameter in flow control, the optimal values of GF mounting location and GF mounting angle are fixed as X=1.00 and $\varphi=90^0$. With the increase in the GF height H from 0.01 to 0.1, the figure 11 shows an increment in turning angle compared to the baseline cascade. On the other hand, the total loss coefficient marks also a rise when the GF height increases, as illustrated in right of the fig.11.

In front of this situation the value H=0.02 of the GF height is adopted as the optimum because beyond this value the level of total losses is abruptly increased to $\delta(\varpi)=10\%$ for the configuration H=0.03. Moreover, the cascade with GF height H=0.01 has a negligible enhancement in total loss coefficient and 2 degree of deflection less than the optimal case. As cited in the literature review that the optimal flap height should be between the values 1 and 2 percent of the

chord for admissible losses, the predicted results in Fig. 11 confirm this result and are found to match very closely with the majority of works carried out in the domain of flow control by Gurney flap [4,8]. After this parametric study, the best controlled configuration is identified by the mounting location X=1.00, the mounting angle $\varphi=90^0$ and the height value H=0.02.

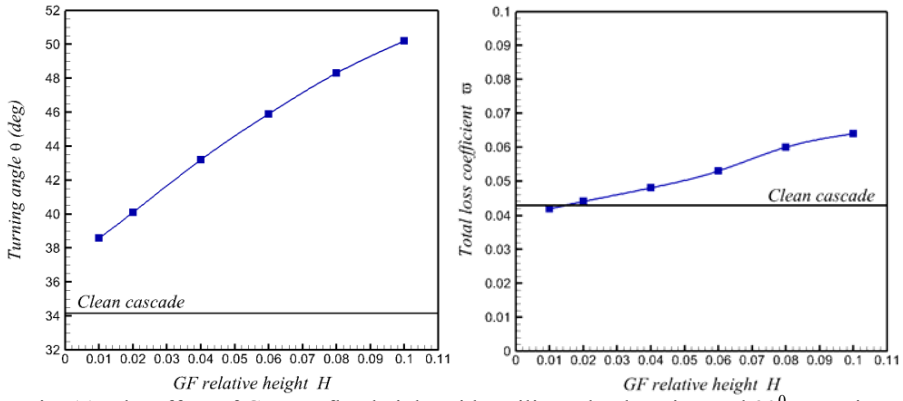

Fig. 11. The effect of Gurney flap height with trailing edge location and 90^0 mounting angle on turning angle-left and total loss pressure-right

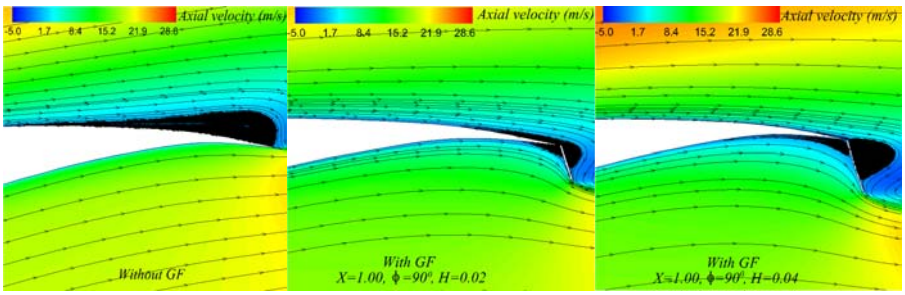

Fig. 12. Axial velocity contours and streamlines for clean and controlled cascades for two heights (H=0.02 and 0.04)

The Fig. 13 illustrates the evolution of static pressure coefficient for both optimal flapped blade rows and unflapped cascade. The results indicate a pressure increase on the intrados and suction increase on the extrados using the best Gurney flap, which lead to ameliorate the turning angle. Concerning the variation of the first circumferential derivative of axial velocity at suction surface between clean and best flapped blading, it seems that the separation zone developed on the extrados is delayed when the GF is used.

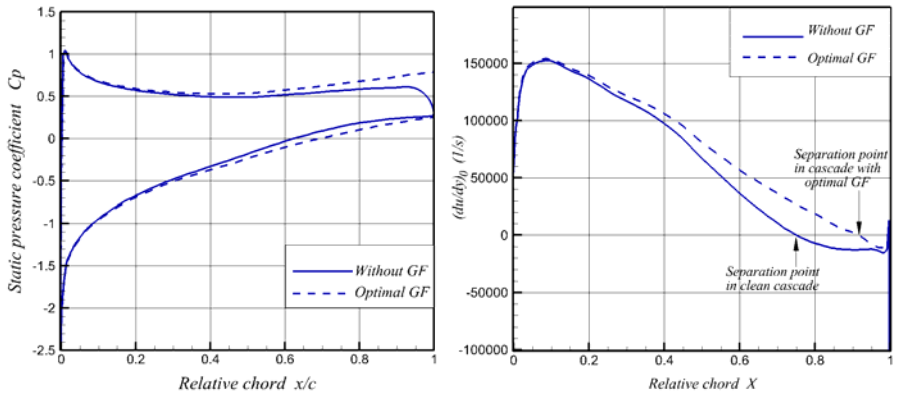

Fig. 13. Comparison between clean and best controlled cascade of, static pressure coefficient on blade surface-left and the first circumferential derivative of axial velocity at suction surface-right

4. Results over a range between the design and stall conditions

The clean cascades are rebuilt once again and provided with the best Gurney flap configuration. In fact, with an inlet flow angle $\beta_1=45^0$ and eight stagger angles $\lambda=18^0$, 20^0, 22^0, 24^0, 28^0, 30^0, 34^0 and 38^0 a wide range of angle of attack between 7^0 and 27^0 is obtained in order to document over it, through the figure 14, the variation of turning angle and total loss coefficient for both clean and controlled cascades. The experimental data of Emery is added to show the good evolution of the numerical results. Concerning the total losses, it seems that the control using Gurney flap provokes an increase in total pressure loss coefficient over the entire range; especially around the design point. The relative rise in the total loss coefficient $\delta(\varpi)$ is approximately 16% and 2% at design and stall angles, respectively. In the other hand, the turning angle values between both cascades flapped and unflapped are improved with approximately 7.4^0 to 9^0 over the chosen range. Therefore, the Gurney flap marks its benefit by enhancing the flow deflection. Contrariwise, the expected rise in the loss coefficient, particularly in the range without separated boundary layer, exceeds the tolerable limits. Albeit this, the use of Gurney flap in semi passive manner gives us a better solution; it might be possible to deploy the GF in the stalled operation and retract it in the operation without separated boundary layer.

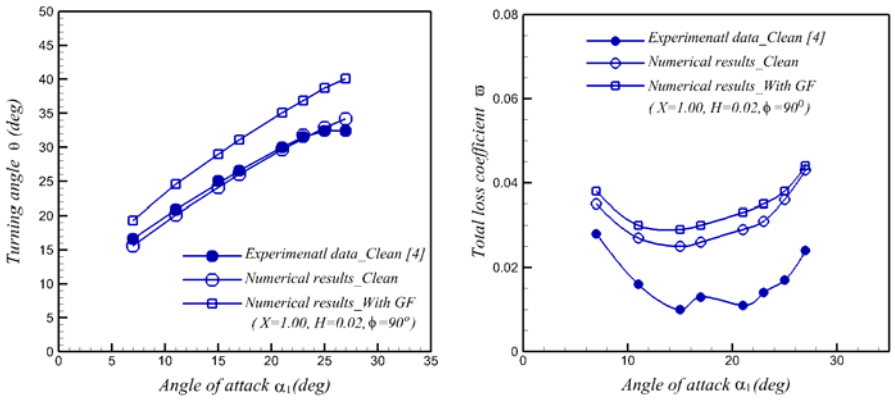

Fig.14. Evolution of turning angle (left) and total loss coefficient (right) with the angle of attack for cascades without and with optimal Gurney flap

Fig. 15 shows wake velocity at outlet cascade for both design and stall cases corresponding to the angles of attack $\alpha_1=15^0$ and 27^0, respectively. This figure reveals that the momentum deficit in the wake region is higher with optimal flap than of the clean blading and therefore, it confirms that the losses are increased when the GF is used. Moreover, it shows that the wake is shifted downward under the effect of increasing the camber via GF.

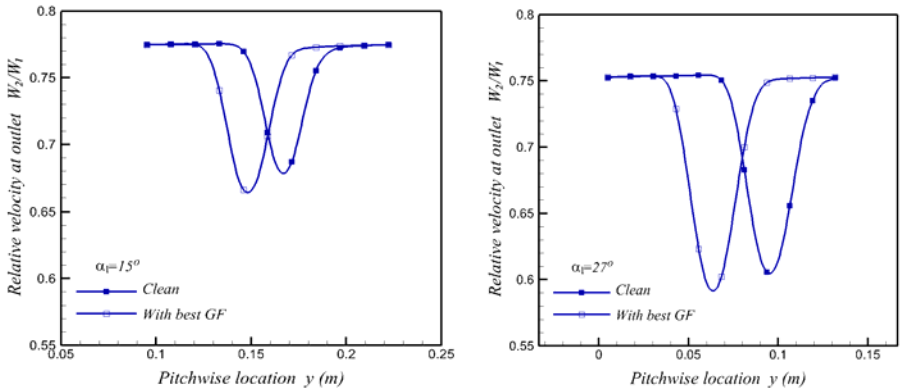

Fig. 15. Evolution of relative velocity in the wake at the outlet for design point (angle of attack $\alpha_1=15^0$)-left and off design point ($\alpha_1=27^0$)-right

5. Conclusions

Passive control with the Gurney flap had been demonstrated on axial compressor linear cascade with highly cambered blading NACA 65(15)10. The numerical experimentations were carried out in order to studying the effect of the control parameters; mounting location, mounting angle and height of the Gurney flap. Based on the stalled configuration, the parametric analysis leads to identify

the optimal cascade. For the Gurney flap to be effective, it must be located at the trailing edge perpendicular to the chord line of blade. Concerning the Gurney flap height, it should be of the order of 2 percent of the chord length. In the chosen range, the obtained results indicate an important enhancement in the turning angle with penalty in total loss coefficient. Moreover, the detachment zone is delayed under effect of the best Gurney flap. In fact, this numerical investigation shows the Gurney flap effects in 2D configuration, which permit us in the future work, to use the optimal GF in three-dimensional cascades in order to explore the GF potential in front of the secondary flows effects.

R E F E R E N C E S

[1]. *R.H. Liebeck,* Design of subsonic aerofoils for high lift, Journal of Aircraft, **vol. 15**, 1978, pp. 547–561.

[2]. *R. Myose, S. Hayashibara, I. Heron,* Flow Visualization Study on the Effect of a Gurney Flap in a Low Reynolds Number Compressor Cascade, 6th AIAA Aviation Technology (ATIO), Wichita, Kansas, 2006

[3]. *A. Byerley, O. Stormer, J. Baughn, T. Simon, K. Van Treuren, and J. List,* "Using Gurney Flaps to Control Laminar Separation on Linear Cascade Blades", in ASME., **vol. 125**, 2003, pp.114-120

[4]. *Y. Li, J. Wang, and P. Zhang,* "Effects of Gurney Flaps on a Naca0012 Airfoil", Flow, Turbulence and Combustion, **vol. 68**, 2002, pp. 27-39

[5]. *J.C. Emery, L.J. Herrig, J.R. Erwin, and A.R. Felix*, "Systematic Two-Dimensional Cascade of NACA 65-Series Compressor Blades at low Speeds" , NASA report 1368, 1958.

[6]. *J.H. Horlock,* Axial Flow Compressors, Fluid Dynamics and Thermodynamics, Robert E. Krieger Publishing Co., 1973.

[7]. *J.J.Wang, Y.C. Li, K.S. Choi,* 2008, "Gurney Flap-Lift enhancement, mechanisms and applications", Progress in aerospace Sciences, **vol.44**, 2008, pp. 22-47

[8]. *I.H. Abbot, and A.E. Von Doenhoff, Theory* of Wing Sections, Dover Publication Inc., 1959.